The Air-Sea Interface, Radio and Acoustic Sensing, Turbulence and Wave Dynamics, Marseille, 24-30. June 1993, edited by M. A. Donelan, W. H. Hui and W. J. Plant
RSMAS, University of Miami, 1996, doi: 10.5281/zenodo.13994

THE VIERS SCATTEROMETER ALGORITHM

J. A. M. Janssen, C. J. Calkoen, D. van Halsema, B. Jähne, P. A. E. M. Janssen, W. A. Oost, P. Snoeij, J. Vogelzang and H. Wallbrink
Royal Netherlands Meteorological Institute (KNMI), 3730 AE De Bilt, The Netherlands

Abstract. Various backscatter theories have been investigated in a tank experiment. A simple two-scale model performed better than other more complicated models. In combination with an air-sea interaction module the two-scale model provides the physical basis for the present Viers scatterometer algorithm. A first test of the algorithm with ECMWF and ERS-1 data shows that the model σ_0 values agree with those of the satellite. At low winds the algorithm performs better than the operational CMOD4.

1 Overview

Viers-1 is a joint research project of the following institutes: the Royal Netherlands Meteorological Institute (KNMI), Delft Hydraulics, the Laboratory for Telecommunication and Remote Sensing Technology of the Delft University of Technology, the University of Heidelberg, the Physics and Electronic Laboratory of TNO (FEL-TNO), and Rijkswaterstaat, Tidal Waters Division. Financial support for the contribution of the Dutch institutes is provided by the Netherlands Remote Sensing Board (BCRS), the German contribution has been made possible by a grant from the state of Baden Württemberg and the European Community.

The objective of Viers-1 is to understand the physics of the scatterometer. To that end three major experiments have been performed: a tank, an outdoor flume and a field experiment (VIERS, 1992). In order to interpret the experimental results a physical model was set up. Such a model relates the radar backscatter to the wind and consists of a backscatter and an air-sea interaction module.

Four alternative backscatter modules have been developed and tested. In the tank experiment 2-D wavenumber spectra $W(\vec{k})$ could be carefully measured with the new ISG technique (Jähne and Riemer, 1990). The backscatter modules could thus be tested by comparing the measured σ_0 with the model values obtained by inputting the measured $W(\vec{k})$. On the basis of this test we have chosen the two-scale module as the prime backscatter module in the full Viers scatterometer algorithm. See section 2 for more details.

The air-sea interaction module of the Viers algorithm has been developed by the authors. It provides at the output side the 2-D spectrum $W(\vec{k})$; input parameters are wind speed and direction and wave age. The latter parameter describes the stage of development of the sea waves. Details will be given in section 3.

The Viers algorithm has been subjected to a first test with ERS-1 data: it performs better than the operational model CMOD4 at low wind speeds. See section 4.

2 Comparison of backscatter models

The following backscatter models were investigated.

- **Small Perturbation Method** (SPM). This method, developed by Rice, leads to the well-known Bragg expression for the radar backscatter.
- **Two-Scale Model** (TSc). In this approach the sea is composed of independent slightly rough patches. The patches are tilted by long waves and the net backscatter is the average backscatter for a single patch (average over long wave slopes). Our first implementation was based on the work of Donelan and Pierson (1987). Their model performs satisfactorily at sea, but it turned out that in the laboratory tank at high wind speed the VV prediction of the model was too high as was the difference between HH and VV. Also for other reasons it was decided to make another implementation. An essential parameter is k_c which separates the long tilting waves from the short Bragg waves. In the Viers implementation of the two-scale model this parameter is determined by the relation $4k_r^2\sigma_H^2 = \beta$, where k_r is the radar wavenumber, β is a constant of the order of 0.1, and the variance σ_H^2 is given by $\sigma_H^2 = \int_0^{2\pi}\int_{k_c}^{\infty} W(k,\alpha)kdkd\alpha$. Only waves with $k > k_c$ may act as Bragg scatterers. Waves with $k < k_c$ violate the criteria for application of the SPM and therefore they are assumed not to contribute to the Bragg scattering. They may, however, contribute to the specular reflection, which is also included.
- **Holliday model** (HSW). This model and the next two are approximations to the full Maxwell equations. HSW is polarization independent and therefore not further discussed.
- **IEM model by Fung and Pan** (IEM).
- **Full wave model by Bahar** (Bah).

The relation between σ_0 and $W(\vec{k}) = W_r(k)W_a(\alpha)$ in the last three models involves several integral equations. In order to get an efficient algorithm the radial and angular part of the spectrum are assumed separable and parameterized as

$$W_r(k) = \frac{Bk^4}{k_p^8 + k^8} \qquad W_a(\alpha) = \frac{1}{2\pi}(1 + 2a_2\cos 2(\alpha - \alpha_W))$$

It turned out that measured ISG spectra could very well be represented in this parametrised form, especially in the Bragg region (accuracy better than 20 per cent).

In Figures 1 and 2 measurements and model results for σ_0 are depicted as a function of incidence angle for HH and VV polarization respectively. The wind speed is fixed ($u_* = 0.367$ m/s) as is the look direction (upwind). In Figures 3 and 4 the same is done, but now the wind speed varies, while the incidence angle is fixed at 45^0 and the look direction is upwind. The model results were produced by first determining the parameters k_p, B and a_2 ($\alpha_W = 0$ in the upwind direction) and subsequently feeding the parametrized spectrum into the backscatter module. The models SPM, TSc, IEM and Bah have full, dashed,

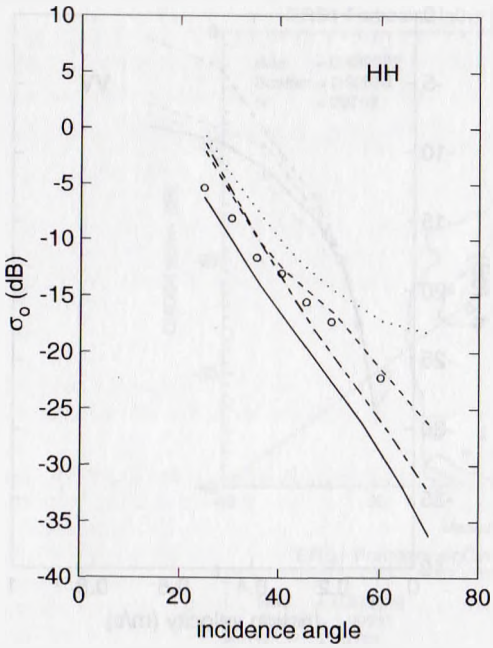

Fig. 1. Measurements and model results of σ_o versus incidence angle at HH polarization. The models SPM, TSc, IEM, and Bah are denoted by full, dashed, dotted, and dash-dotted lines respectively.

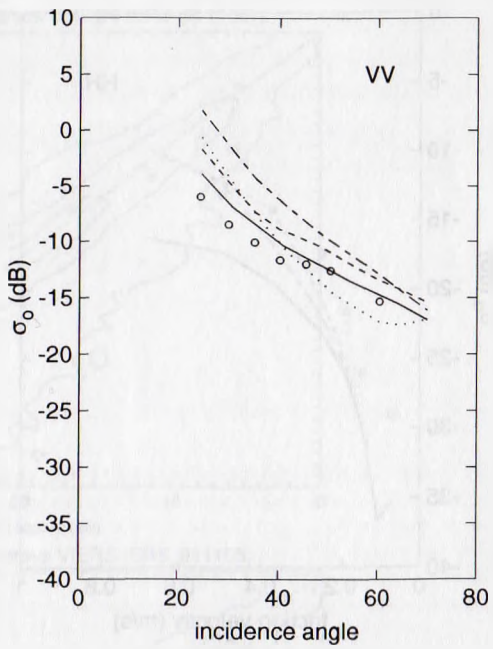

Fig. 2. Measurements and model results of σ_o versus incidence angle at VV polarization. The models SPM, TSc, IEM, and Bah are denoted by full, dashed, dotted, and dash-dotted lines respectively.

dotted and dash-dotted lines respectively. There is no perfect model, but the two-scale model performs relatively well.

3 Air-sea interaction module

The air-sea interaction module consists of three sub modules. The wind module calculates the friction velocity given the wind speed (U_{10}), wave age, and air-sea temperature difference. The sea-state dependent roughness length found in the HEXOS experiment (Smith *et al.*, 1992) has been incorporated. In the two wave modules (for gravity and gravity-capillary waves) the 2-D wavenumber and frequency spectra are assumed separable; the angular part is parametrised as follows.

$$W_a(\alpha) = \frac{1}{2\pi}(1 + 2a_2 \cos(\alpha - \alpha_W)) \qquad a_2 = 0.175 + 0.075u_*$$

The radial part for the gravity waves ($k < k_0, f < f_0$) depends on friction velocity and wave age and is in the present sea version (in a wave tank one needs another peak parametrisation) a Jonswap spectrum (Hasselmann *et al.*, 1973) with the following parameters:

$$\gamma = 3.3 \qquad \sigma = 0.08 \qquad \alpha = 0.52(c_p/u_*)^{-1.41} \qquad f_p = \frac{g}{2\pi u_*}(c_p/u_*)^{-1}$$

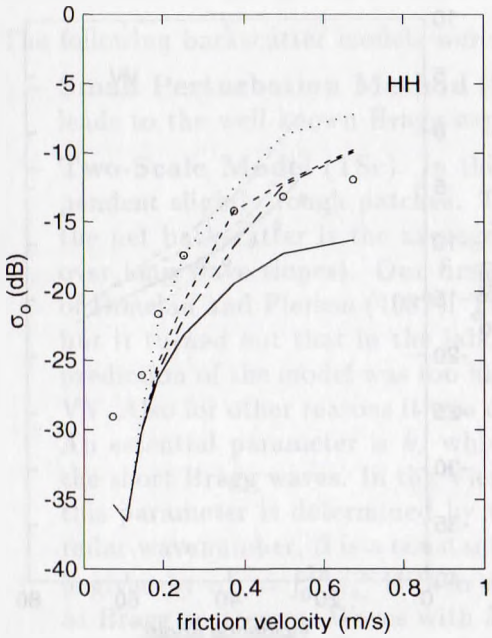

Fig. 3. Measurements and model results of σ_o versus u_* at HH polarization. The models SPM, TSc, IEM, and Bah are denoted by full, dashed, dotted, and dash-dotted lines respectively.

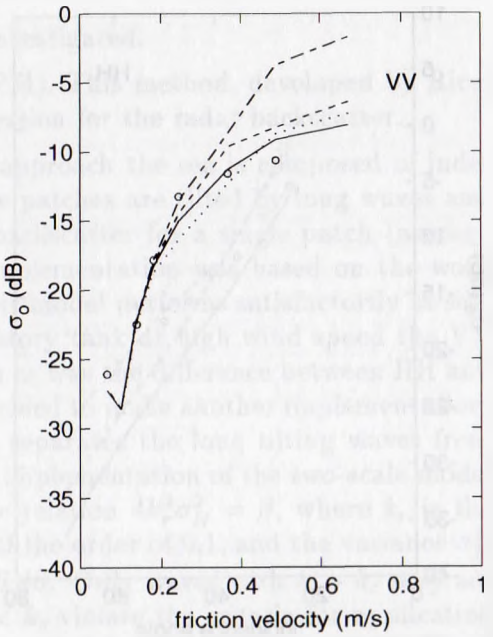

Fig. 4. Measurements and model results of σ_o versus u_* at VV polarization. The models SPM, TSc, IEM, and Bah are denoted by full, dashed, dotted, and dash-dotted lines respectively.

In a future version it is intended to use ocean wave spectra calculated by WAM.

Due to their short response time the 1-D spectrum for the gravity-capillary waves ($k > k_0$) is found by setting the total energy source equal zero: $S = S_{in} + S_{nl} + S_{br} + S_{vis+sl} = 0$. As wind input we use the expression proposed by Plant (1982), modified by Janssen's (1982) quasi-linear effect. Breaking is modelled according to Komen *et al.* (1984) with $n = 2$. The enhancement of viscous damping by slicks is due to the Marangoni effect (Alpers and Hühnerfuss, 1989). For the nonlinear interactions a model by P. Janssen has been used. S_{nl} is written as the divergence of the energy flux, which is assumed to be quadratic (3-wave) and/or cubic (4-wave) in the spectrum.

The equation $S = 0$ is a first-order differential equation in the 1-D spectrum. The boundary condition is provided by the energy flux at $k = k_0$. Good spectra are obtained if one puts $k_0 = g/u_*^2$.

4 Validation against ERS-1 data

Do the resulting model σ_0 values agree with those measured by ERS-1 if one feeds collocated ECMWF wind and wave data into the Viers model? As Figure 5b shows, the answer is yes. Here ERS-1 σ_0 values on one particular day (11/6/91) and for one particular beam (forebeam) are plotted against the cor-

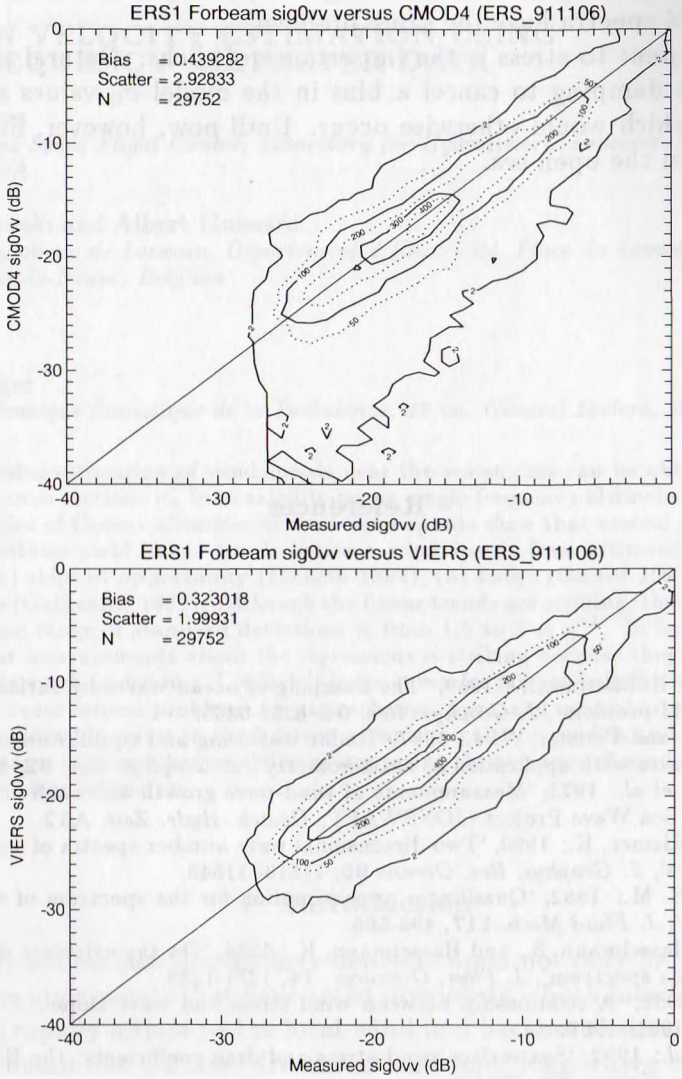

Fig. 5. a) CMOD4 model σ_o versus ERS-1 σ_o, b) VIERS model σ_o versus ERS-1 σ_o.

responding model σ_0 values. The numbers at the contours lines denote the density of points (number/dB^2). In Figure 5a the present operational algorithm CMOD4 has been subjected to the same test. Clearly, CMOD4 has trouble with the low wind speeds ($U_{10} < 4$). The picture given by Figure 5 is generic as there is no change in the scatterplots if one takes another day or beam.

The result of Figure 5b (no bias, low scatter) looks impressive indeed. One should bear in mind, however, the following. The rms slopes of the tilting waves, as calculated by the present air-sea interaction module, are quite low. If they are used by the backscatter module, the model σ_0 values become too low. In order to avoid this bias the rms slopes are artificially enhanced (40 per

cent) before they are passed to the backscatter module. It will be investigated whether WAM spectra have the same problem.

A second point to stress is the importance of slicks. Natural slicks already give sufficient damping to cancel a bias in the model σ_0 values at low winds ($U_{10} < 10$), which would otherwise occur. Until now, however, little is known about slicks on the open sea.

References

Alpers, W., and Hühnerfuss,H.: 1989, 'The damping of ocean waves by surface films: a new look at an old problem', *J. Geophys. Res.* **94**, 6251-6265.

Donelan, M. A., and Pierson, W. J.: 1987, 'Radar scattering and equilibrium ranges in wind-generated waves with application to scatterometry', *J. Geophys. Res.* **92**, 4971-5029.

Hasselmann, K. *et al.*: 1973, 'Measurements of wind-wave growth and swell decay during the Joint North Sea Wave Project (JONSWAP)', *Deutch. Hydr. Zeit.* **A12**.

Jähne, B., and Riemer, K.: 1990, 'Two-dimensional wave number spectra of small-scale water surface waves', *J. Geophys. Res. Oceans* **95**, 11513- 11546.

Janssen, P. A. E. M.: 1982, 'Quasilinear approximation for the spectrum of wind-generated water waves', *J. Fluid Mech.* **117**, 493-506.

Komen, G. J., Hasselmann, S., and Hasselmann, K.: 1984, 'On the existence of a fully developed wind-sea spectrum', *J. Phys. Oceanogr.* **14**, 1271-1285.

Plant, W. J.: 1982, 'A relationship between wind stress and wave slope', *J. Geophys. Res. Oceans* **87**, 1961- 1967.

Smith, S.D. *et al.*: 1992, 'Sea surface wind stress and drag coefficients: the HEXOS results', *Bound-Layer Meteor.* **60**, 109-142.

VIERS.: 1992, VIERS progress reports 1, 2 and 3. Technical Reports BCRS 89-24 (1989), 90-27 (1990) and 92-24 (1992), KNMI, De Bilt, The Netherlands.